



Research article

Fabrication of FRP/CNT hybrid laminate composites and their effect on interlaminar and mechanical properties

Mateo Duarte¹, Johan A. Oquendo¹, Sebastián Vallejo¹, Johnattan Vargas¹, Yamile Cardona-Maya² and Cesar A. Isaza^{3,*}

¹ Facultad de Ingeniería, Institución Universitaria Pascual Bravo, Medellín, Colombia

² Departamento de Fundamentación básica, Institución Universitaria Pascual Bravo, Medellín, Colombia

³ Departamento de ingeniería mecánica, Facultad de ingeniería, Universidad de Antioquia UdeA, Calle 70 No. 52-21, Medellín, Colombia

* **Correspondence:** Email: cesar.isaza@udea.edu.co.

Abstract: Composites are widely used in different areas of engineering due to their remarkable mechanical properties; however, it has been evidenced that laminated composites exhibit certain vulnerabilities, particularly in interlaminar regions, which can lead to failures. To address this issue, efforts have been made to enhance interlaminar strength, with one notable approach being the incorporation of nano-reinforcements that serve as bridges between the laminate layers. Among these nano-reinforcements, carbon nanotubes (CNTs) have emerged as a highly promising material to mitigate the deficiencies in interlaminar zones. Despite their potential, integrating CNTs into structural laminates presents significant challenges. This research focuses on developing a strategy to effectively incorporate well-dispersed multi-walled carbon nanotubes (MWCNTs) into structural laminate composites to enhance interlaminar toughness. The study explored three different processes for integrating MWCNTs: hand lay-up, vacuum bagging, and liquid resin infusion, each with varying percentages of MWCNT addition. The aim was to determine the most efficient method for achieving uniform dispersion and improved mechanical properties. The results of this investigation demonstrated that well-dispersed MWCNTs significantly enhance the interlaminar and overall mechanical properties of composites. Each method showed varying degrees of success, but the overarching conclusion is clear: MWCNTs, when properly integrated, offer a viable solution to the inherent weaknesses of laminated composites. This advancement holds substantial promise for the future of composite materials, particularly in applications requiring enhanced durability and strength. The findings pave

the way for further research and development in optimizing nano-reinforcement techniques, ultimately contributing to the creation of more robust and reliable composite structures.

Keywords: hybrid nanocomposites; glass fiber; carbon nanotubes; mechanical properties

1. Introduction

The need to find new materials that meet specific structural characteristics has driven the development of materials with exceptional mechanical performance, particularly those with a high strength/weight ratio. Fiber-reinforced composites (FRCs) have thus emerged as a significant advancement [1–3], finding applications in industries such as automotive, aerospace, and aeronautics [4], among others [5,6]. In general, FRCs are materials with high strength and modulus compared to their parent materials [7,8]. For this reason, FRCs are extensively utilized for structural components due to their excellent mechanical properties. A notable limitation of these materials is their relatively low through-thickness properties, which makes them susceptible to delamination upon impact and limits their application viability. The failure mechanisms of these materials can be divided into intralaminar failure and interlaminar failure. Intralaminar failure takes place within a single layer and involves fiber breakage, detachment between the fiber and the matrix, fiber pull-out, and matrix breakage. On the other hand, interlaminar failure, which is more typical, refers to delamination occurring at the interface between adjacent layers [9]. Therefore, in laminated composites, the interlaminar behavior, such as low interfacial adhesion and low interlaminar strength, causes a decrease in the final mechanical properties of the composite [10]. Consequently, there is a need to enhance the interfacial properties of FRCs in large-scale engineering applications. For this reason, several authors have proposed two possible approaches: modeling predictive approaches and manufacturing solutions. The first one involves the development of analytical and numerical models to predict the mechanical response of debonding issues in multilayered composites. For example, Greco et al. [11] performed a novel approach to predict debonding or fracture in multilayered composite beams, allowing the use of Arbitrary Lagrangian-Eulerian (ALE) formulation combined with delamination fracture mechanics to simulate crack propagation. Moreover, similar proposals have been applied in multiple applications such as concrete or steel beams strengthened/repared with externally bonded composite laminated plates [12] and graphite/epoxy composite materials [13]. The manufacturing solutions include fiber hybridization [14], fiber refinement [15], nanofibers [16], and, more recently, the use of carbon nanotubes (CNTs) [17] to increase the interlaminar strength of FRCs. CNTs have been employed for toughening FRC composites; their integration techniques in polymer matrices can be classified as mixing in bulk resin [18], in situ CNTs growth [19,20], physical transfer of the CNTs particles [21], and CNTs interleaving technique [22].

Once the nano-reinforcements have been incorporated into the matrix and/or fibers, the composites can be fabricated using conventional manufacturing processes such as hand lay-up [23], liquid resin infusion [24], and vacuum bag [25], among others.

Several authors have integrated CNTs into carbon fiber polymer composites, demonstrating good mechanical performance. Kepple et al. [26] functionalized carbon fibers with CNTs using an in situ process. Results revealed that CNTs improved the fracture toughness of the composites. Similarly, Godara et al. [27] manufactured CNTs/carbon fiber/epoxy prepregs using high-shear calendaring

equipment and the drum winder technique, and the results evidenced a noticeable improvement in crack initiation and propagation energy of the CNTs-toughened composites. Davis and Whelan [28] demonstrated that fluorine-functionalized CNTs can strengthen laminated composites and increase their mode-II interlaminar fracture toughness by 27%. Yu et al. [29] incorporated multi-walled carbon nanotubes (MWCNTs) functionalized with silanes on the surface of carbon fibers to enhance their interfacial adhesion with the epoxy matrix. Micro-adhesion test results showed that the interfacial shear strength of the laminates with MWCNTs increased by 26% compared to the reference laminates. Subsequently, Wicks et al. [30] demonstrated that the use of fibers with aligned CNTs on their surfaces as reinforcement for laminated composites improves their inter and intralaminar fracture properties. The addition of aligned CNTs has been shown to improve the steady-state mode-I fracture toughness of laminated composites. Yokozeki et al. [31] investigated the mechanical properties of laminated composites manufactured based on carbon fiber prepreps and epoxy resin modified with CNTs. The results indicated significant improvements in the stiffness and mechanical strength of the laminate composites.

Although most of the studies focus on hybrid CNTs/carbon fiber/matrix composites, some authors have explored the use of glass fibers. Sheth et al. [32] performed FRCs using the hand lay-up and hot press technique, incorporating CNTs as a sizing between the glass fiber and polymeric matrix. The authors used the mixing technique to integrate the CNTs. In general, the results showed an improvement in the mechanical properties of FRCs with a maximum of 1 wt.% of CNTs, followed by a decrease due to the potential agglomeration of the CNTs within the matrix. Tensile strength in FRCs with 1 wt.% of CNTs added to the matrix increased by approximately 10% compared to fiber composite without CNTs; furthermore, a similar behavior was observed for the flexural strength. Similarly, Rathore et al. [33] proposed the use of MWCNTs for manufacturing hybrid composites. The authors dispersed the MWCNTs using the magnetic stirring process in an acetone solution, which was later mixed with an epoxy matrix and sonicated. Finally, the composite material was made using the hand lay-up technique with 14 layers (fabrics) and the consolidation of the material was obtained through hot press. Despite the promising results, the authors acknowledge that several critical aspects still require optimization, including dispersion stability. Some studies have indicated that the incorporation of CNTs into fiber-reinforced polymeric composites can adversely affect their interlaminar fracture toughness due to the tendency of CNTs to form clusters [34,35]. However, most of the research demonstrates a positive effect on the interlaminar fracture properties of laminated composites through the successful incorporation of nanomaterials into their matrix, fiber, and interface. Finally, Sunil and Dikshit [36] reported a novel and practical technique for dispersing MWCNTs onto woven carbon fiber-reinforced polymers prepreg. The results demonstrated that the composite exhibited favorable mechanical properties. Furthermore, the technique facilitated the percolation of MWCNTs into the top layers of fibers within the tows.

In this study, we characterized a hybrid composite consisting of MWCNTs embedded in an epoxy matrix reinforced with glass fiber by evaluating its tensile strength and interlaminar strength. Additionally, we employed nanomechanical characterization through nanoindentation to assess and quantify the dispersion of MWCNTs within the polymeric matrix.

2. Materials and methods

2.1. Raw materials

Epoxy resin and woven roving fiberglass with a weight of 800 g/m² were supplied by SUMIGLAS S.A. Additionally, MWCNTs with a purity of 98% were supplied by Nanostructured & Amorphous Materials Inc. These MWCNTs have lengths ranging from 30 to 50 μm, inner diameters ranging from 10 to 20 nm, and outer diameters between 10 and 40 nm. The MWCNTs used showed some imperfections (amorphous carbon and bamboo-type defects) and catalytic particles (nickel), whose defects can enhance interactions with the matrix materials. Figure 1a illustrates the morphological characteristics of the MWCNTs used in this study; Figure 1b shows a detailed image of the CNTs evidencing their concentric graphene layer walls and the nickel nanoparticles used as precursors for the synthesis of the CNTs.

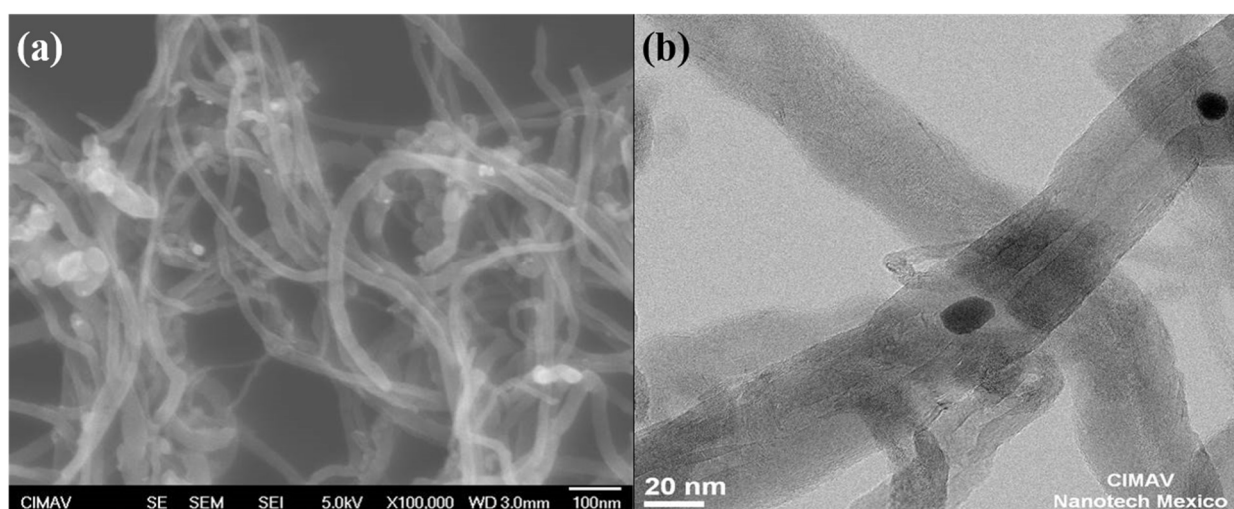


Figure 1. MWCNTs used for manufacturing hybrid composites. (a) Scanning electron microscope (SEM) image, (b) transmission electron microscope (TEM) image.

2.2. Composite synthesis

The hybrid composites were manufactured in two steps, as shown in Figure 2. The first step involved dispersing the MWCNTs (0.5 wt.% and 1 wt.%) within the epoxy matrix using an ultrasonic lance (Figure 2a). To achieve a well-dispersed mixture of MWCNTs in the epoxy matrix, a factorial experiment was conducted, considering variables such as MWCNTs percentage, agitation energy, and agitation time. The process for the CNTs dispersion is as follows: The sample was homogenized by magnetic stirring and subjected to ultrasonic dispersion for 3 and 4 h for MWCNTs weight percentages of 0.5% and 1%, respectively. A variation in the power percentage between 25% and 50% was used for this purpose. Finally, the sample was left to cure for 24 h; then, the composite was removed from the mold and placed in an oven to complete the curing process at 70 °C for 1 h.

The second step involved manufacturing the hybrid composite. This process included stacking three sheets of glass fiber with orientation angles of 0, 45, and 90° (see Figure 2). Subsequently, three

different manufacturing techniques were employed for composite synthesis: hand lay-up, liquid resin infusion, and vacuum bag, as illustrated in Figure 2b.

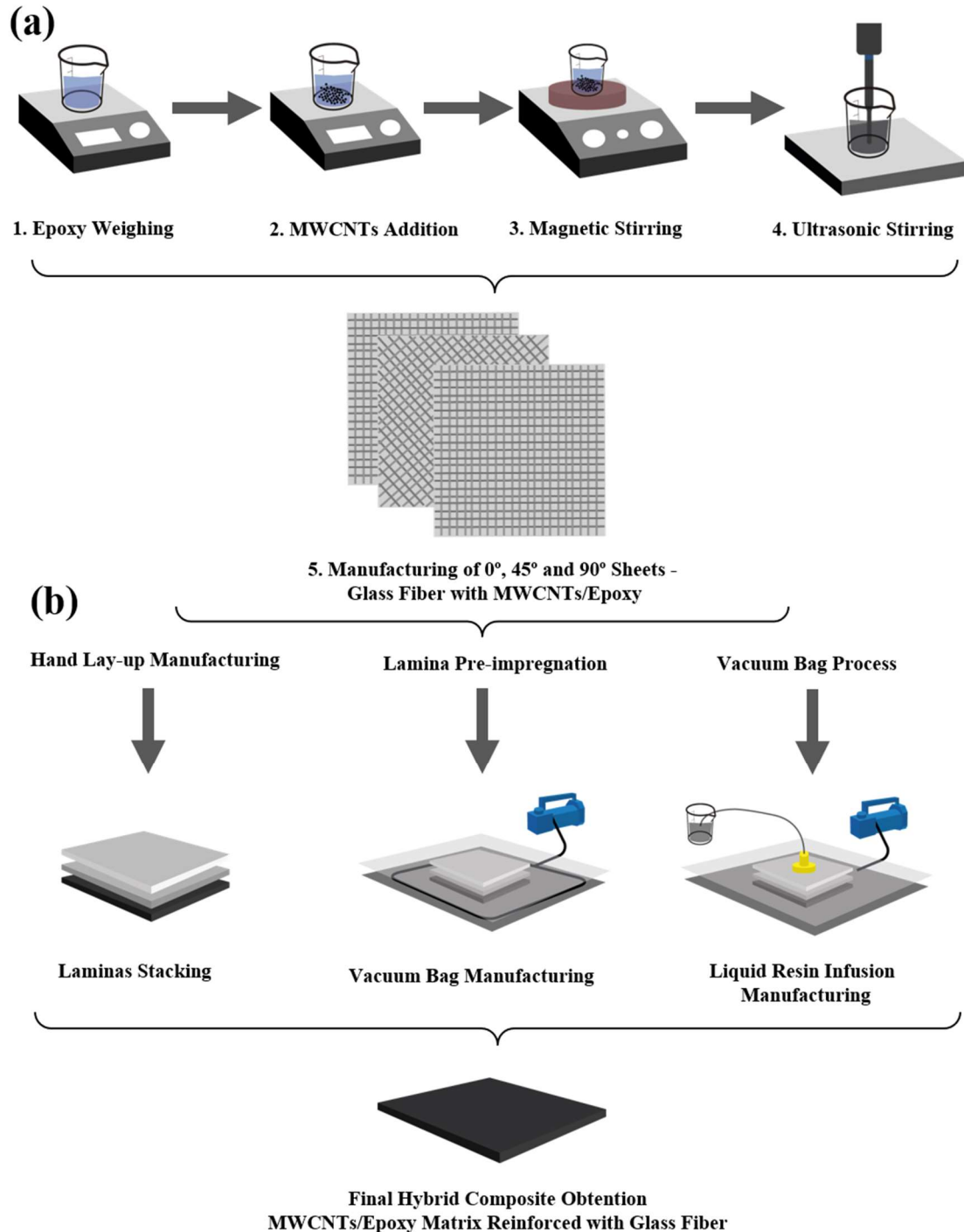


Figure 2. Hybrid composites preparation. (a) MWCNTs dispersion in polymeric matrix and (b) composite manufacturing.

2.3. MWCNTs dispersion qualification on polymer matrix composites nano-reinforced

To assess the dispersion effect of the MWCNTs into the polymeric matrix, tensile and nanoindentation tests were conducted. Tensile tests were performed using a Shimadzu GX series tension machine at a rate of 10 mm/min, following the ASTM D239 standard. Nanoindentation tests were carried out in an IBIS Authority Fischer-Cripps nanoindenter using a peak load of 5 mN. The bulk mechanical properties of epoxy/MWCNTs composites were obtained.

2.4. MWCNTS dispersion quantification on polymer matrix composites nano-reinforced

For dispersion quantification, a modulus mapping was carried out using an IBIS Authority Fischer-Cripps nanoindenter. The mapping area was $3 \times 3 \mu\text{m}^2$ with a maximum load of 0.8 mN, and the separations between indentations were 300 nm. The generated mapping was utilized to identify the changes in mechanical properties in the delimited area. Furthermore, the obtained images were divided into 10×10 grid lines, both horizontally and vertically, to observe the nearest MWCNTs and their measurements at each grid intersection. Figure 3 illustrates the methodology for modulus mapping by nanoindentation.

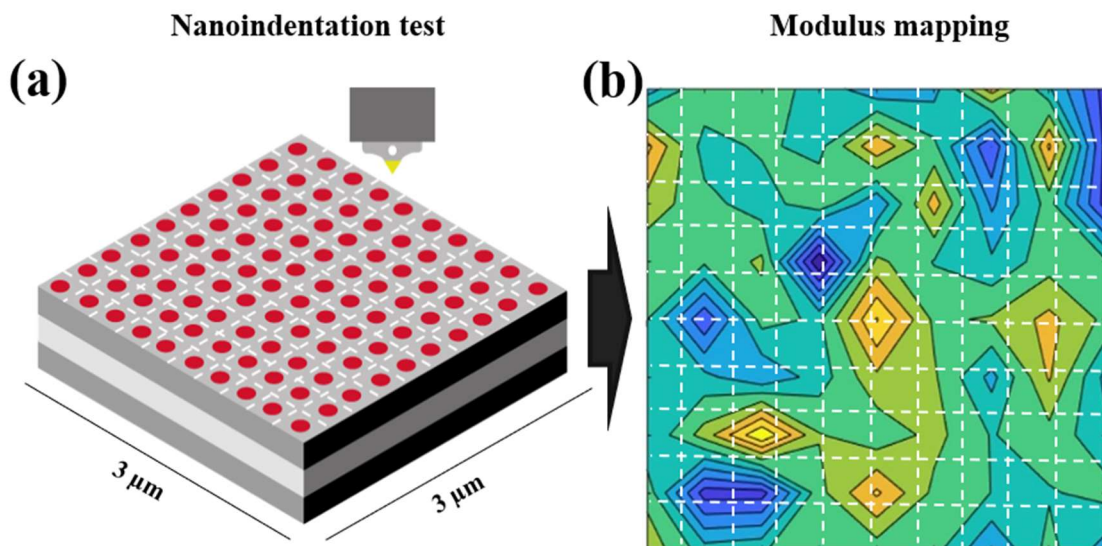


Figure 3. Quantification methodology for Epoxy/MWCNTs. (a) Nanoindentation test and (b) modulus mapping.

These data were analyzed using the statistical distribution model shown in Eq 1.

$$f(x) = \begin{cases} \frac{1}{xn\sqrt{2\pi}} e^{-\frac{1}{2}\left(\frac{\ln x - m}{n}\right)^2} & (x > 0) \\ 0 & (x \leq 0) \end{cases} \quad (1)$$

where

$$m = \ln \frac{\mu^2}{\sqrt{\mu^2 + \sigma^2}} \text{ and } n = \sqrt{\ln \frac{\mu^2 + \sigma^2}{\mu^2}}$$

In which x is the free path distance, μ is the dispersion average, and σ is the standard deviation for the free-path distance measured.

For dispersion quantification, a dispersion parameter, $D_{0.1}$, defined as the probability of the free-path distance distribution, was set in the range of 0.9–1.1 μ . The $D_{0.1}$ is formularized as in Eq 2.

$$D_{0.1} = 1.153910^{-2} + 7.5933 \times 10^{-2} \times \left(\frac{\mu}{\sigma}\right) + 6.6838 \times 10^{-4} \times \left(\frac{\mu}{\sigma}\right)^2 - 1.9169 \times 10^{-4} \times \left(\frac{\mu}{\sigma}\right)^3 + 3.9201 \times 10^{-6} \times \left(\frac{\mu}{\sigma}\right)^4 \quad (2)$$

Since in this method, $D_{0.1}$ is deduced from the free-path distance distribution, a higher $D_{0.1}$ value indicates more spacing data close to the mean μ . A dispersion of 100% means that all the reinforcements are equally spaced, i.e., different percentages of the addition of nano-reinforcements can have the same values as the $D_{0.1}$ parameter.

2.5. Tensile strength characterization of hybrid composites

The tensile test was conducted using a Shimadzu series Gx testing machine at a loading rate of 2 mm/min at room temperature. Samples' dimensions were 250 × 25 mm, following the ASTM D3039 standard for the tensile testing of fiber-reinforced composites. Testing was performed at room temperature (23 °C), and tensile load was applied until failure. The strength was determined from peak load at failure, and five samples were tested.

2.6. Interlaminar strength characterization of hybrid composites

For apparent interlaminar shear strength characterization of the hybrid composites, a short beam shear (three-point bending) test was carried out in a Shimadzu Gx series testing machine with a 5 kN load cell with a crosshead speed of 1 mm/min. The test and calculation of the shear strength were performed following the ASTM D 2344 standard. Eq 3 allows computing the apparent interlaminar shear strength.

$$\tau = \frac{3P}{4bh} \quad (3)$$

where τ is the maximum interlaminar shear strength at failure, P is the applied load, b is the width of the sample, and h is the thickness of the sample.

This method, following ASTM D2344 standard, provides an evaluation of the interlaminar performance, crucial for understanding the resistance to delamination in composites. The test quantifies the impact of nano-reinforcements on the interfacial cohesion of the composite, reflecting improvements in shear strength due to enhanced matrix properties.

2.7. Microscopy analysis

Optical and electronic microscopy analyses were conducted to determine the failure behavior of composite materials. For optical analysis, an optical stereoscope Nikon SMZ1500 with a light source NI-150 was utilized. Additionally, Nis Elements software was used to capture micrographs. To analyze crack growth and the influence of MWCNTs in the mechanical response of the composites, a Jeol 59100 SEM was used.

3. Results and discussion

3.1. Dispersion qualification on polymer matrix composites nano-reinforced

The dispersion qualification was carried out through nanoindentation and tension tests, as described in the methodology section. Figure 4 presents the results of the nanoindentation tests, revealing that the modulus of elasticity varies between 3.5 and 4.5 GPa (Figure 4a) for all manufacturing conditions. Nonetheless, an increase in the mechanical property is observed for the samples with a higher amount of MWCNTs (1 wt.%), and an improvement in the mechanical property is also noted for the sample with higher conditions of energy and time (60 W and 4 h). This trend is also evidenced for the sample with 0.5 wt.% of added MWCNTs. Figure 4b shows a similar behavior for hardness, indicating an influence from the higher energy and time conditions used during MWCNTs dispersion into the epoxy resin.

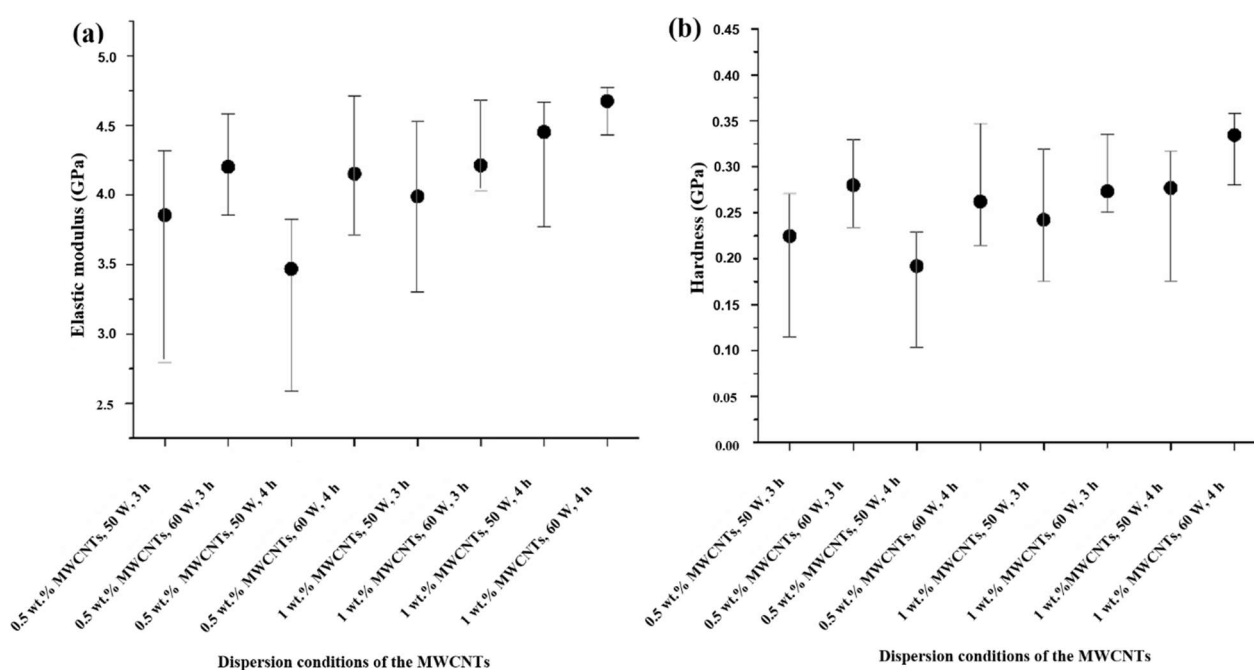


Figure 4. Nanoindentation analysis for polymer matrix composites nano-reinforced: (a) elastic modulus and (b) hardness.

Similarly, the tension tests reveal an influence of MWCNT content into the polymeric matrix, demonstrating that polymer reinforced with 1 wt.% MWCNT exhibits better behavior for the elastic modulus and yield strength, as observed in Figure 5a,b. Furthermore, the results indicate that the best energy and time conditions are obtained for the sample of 1 wt.% MWCNT, 50 W, and 4 h. These findings align with the trends observed in the nanoindentation tests. Even so, there were differences between the mechanical tests due to the interaction volume; in the nanoindentation test, the mechanical properties were measured in a small volume, allowing for higher mechanical property. The results obtained from both tension and nanoindentation tests are comparable to those reported by other authors. For instance, in a study by Medina et al. [37], polyvinyl alcohol reinforced with MWCNTs exhibited an increase in mechanical properties with the addition of CNTs into the polyvinyl alcohol matrix. The authors used an ultrasonic method for MWCNT dispersion, similar to the energy and time conditions employed in this study.

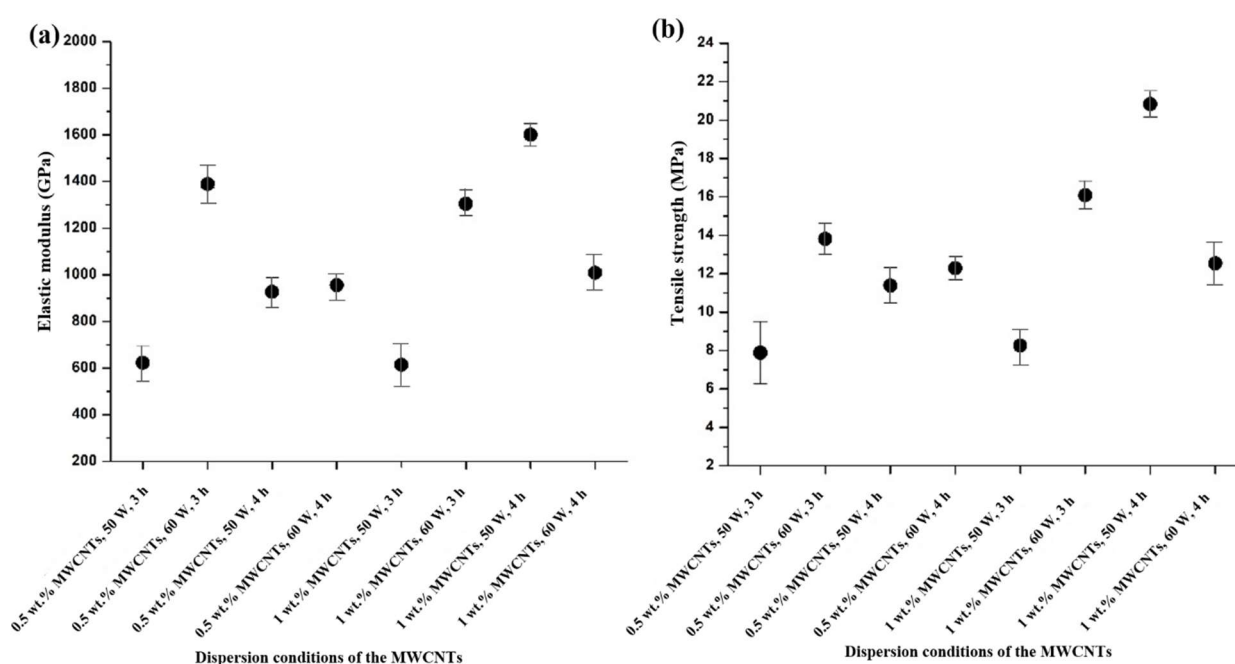


Figure 5. Tensile analysis for polymer matrix composites nano-reinforced: (a) elastic modulus and (b) tensile strength.

3.2. Dispersion quantification on polymer matrix composites nano-reinforced

In Figure 6a,b, characteristic elasticity modulus mappings for the two different percentages of MWCNTs (0.5 wt.% and 1 wt.%) added to the polymeric matrix are observed. The images illustrate how the property changes in a designated study area, where colors indicate the alteration in properties. In this case, blue regions indicate a lower value in the material's property, suggesting no significant impact by the nano-reinforcement. Conversely, yellow regions show a change in property, indicating a potential interaction with the nano-reinforcement. The elasticity modulus values obtained for the two studied composites vary, with the nano-reinforced composite containing 1 wt.% MWCNTs exhibiting a higher property.

It is noteworthy that the images of the two analyzed materials are evenly distributed, indicating good dispersion of the nano-reinforcement in the epoxy matrix. Finally, these mappings allow for an approximate visualization of nano-reinforcement dispersions in the polymeric matrix by using the previously described model. This process involves dividing the images into horizontal and vertical lines and measuring the property change.

On the right side of Figure 6a,b, the distribution graph obtained from measurements of distances between property changes in the mapping image is observed, as detailed in the methodology section. Both composites exhibit a log-normal distribution, and from this, the dispersion parameter $D_{0.1}$ was calculated.

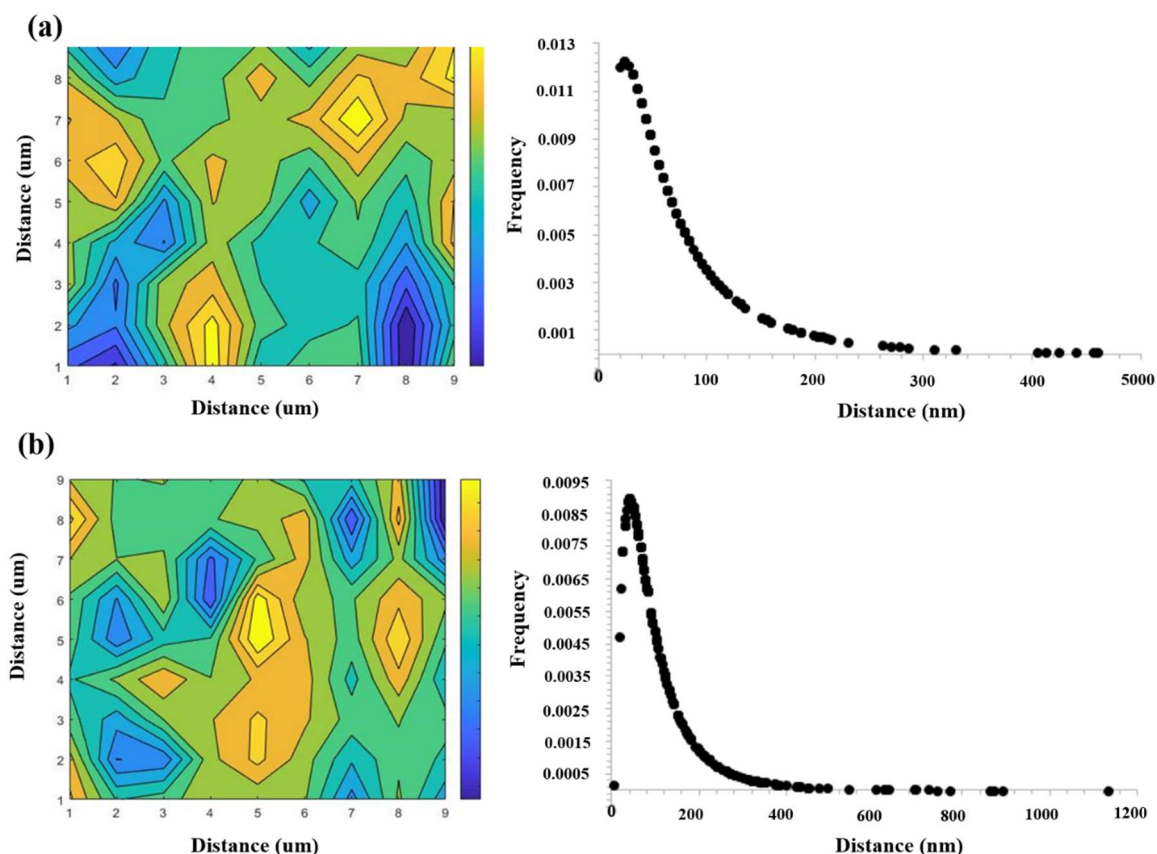


Figure 6. Modulus mapping for hybrid composites nano-reinforced with (a) 0.5 wt.% MWCNTs and (b) 1 wt.% MWCNTs.

The statistical distribution model was utilized to quantify the dispersion of nano-reinforcements in the polymeric matrix. The dispersion degree was quantified for the $D_{0.1}$ parameter from the frequency graph, which provides information on the distances that nano-reinforcements have in the vicinity of the mean. In other words, the $D_{0.1}$ parameter quantifies the percentage of dispersion where most data or measurements among nano-reinforcements are located. With the discussed model and stiffness mappings, it was possible to determine the dispersion of nano-reinforcements in the polymeric matrix. Figure 7 displays the dispersion parameter values for all manufactured materials, indicating that, on average, they have a similar dispersion value due to the dispersion conditions employed. Among all the materials produced, samples with 0.5 wt.% MWCNTs, 60 W, and 3 h, and 1 wt.% MWCNTs, 50 W, and 4 h are selected for the fabrication of hybrid composites.

From these results, the following observations can be made. For the composite reinforced with 0.5 wt.% CNTs, an average distance of 112 nm and a dispersion degree of 7.9% were found. However, most data points are clustered around a distance value close to 30 nm. Similarly, for the composite reinforced with 1 wt.% CNTs, an average distance of 173 nm and a dispersion degree of 9.2% were observed, with most distances clustered around a value close to 48 nm. These results are consistent, as a higher quantity of nano-reinforcements tends to bring them closer within the polymeric matrix. These findings are summarized in Figure 7. It is worth noting that the dispersion results align with those obtained through nanoindentation tests. However, differences with tensile test results are attributed to the measurement size (volumetric) and the manufacturing process (defects).

In general terms, the dispersion conditions used for the manufactured samples show similar behavior. However, upon comparison with other authors [38–40], it is noted that the dispersion percentages range between 3% and 5%. This demonstrates the effective dispersion conditions achieved in this study, which were reflected in the mechanical properties. It should be clarified that the measurement conditions were different; the referenced authors used SEM and TEM images.

Samples	$D_{0.1}$	
0.5 wt.% MWCNTs, 50 W, 4 h	7.0128	
0.5 wt.% MWCNTs, 60 W, 3 h	7.9838	Average distance: 112 μm
0.5 wt.% MWCNTs, 60 W, 4 h	6.5884	
0.5 wt.% MWCNTs, 50 W, 3 h	7.1255	
1 wt.% MWCNTs, 60 W, 3 h	7.1583	
1 wt.% MWCNTs, 50 W, 4 h	9.2340	Average distance: 173 μm
1 wt.% MWCNTs, 60 W, 4 h	7.3142	
1 wt.% MWCNTs, 50 W, 3 h	7.0292	

Figure 7. Dispersion degree parameter for the samples studied.

3.3. Tensile strength characterization of the FRP/MWCNT hybrid laminate composite

The evaluated FRP/MWCNT hybrid laminate composites consider the manufacturing conditions of section 2.2, and the main results for ultimate tensile strength are shown in Figure 8. First, the hand lay-up technique represents the highest increase in tensile strength, wherein the sample with 0.5 wt.% MWCNTs (dash dotted line in Figure 8) showed an approximate improvement of 21% compared to the base sample. Additionally, a decrease in the tensile strength property is observed for 1 wt.% MWCNTs, which could be caused by reinforcement agglomeration or air bubbles, common issues in this technique. Meanwhile, the vacuum bag technique shows a maximum increase in ultimate tensile strength for 1 wt.% MWCNTs, reaching a maximum value of 268 MPa (dotted line in Figure 8). On the other hand, the variations for the liquid resin infusion indicate a low change in the ultimate tensile strength (continuous line in Figure 8). The results obtained align with previous research by Dehrooyeh et al. [17] and Naveed A. Siddiqui [41], where hybrid composites of epoxy/fiberglass/CNTs exhibited

an increase in tensile strength ranging between 10% and 30% compared to the base material. Upon analyzing the overall performance of the manufacturing techniques, it can be concluded that the incremental changes in tensile properties are subtle yet significant. These results may be attributed to the closely matched mechanical properties of both reinforcements (MWCNTs and fiberglass). However, the tensile strength characterization demonstrated the viability of MWCNTs used in hybrid materials to keep mechanical properties and increase the interfacial strength characteristics as discussed in the following section.

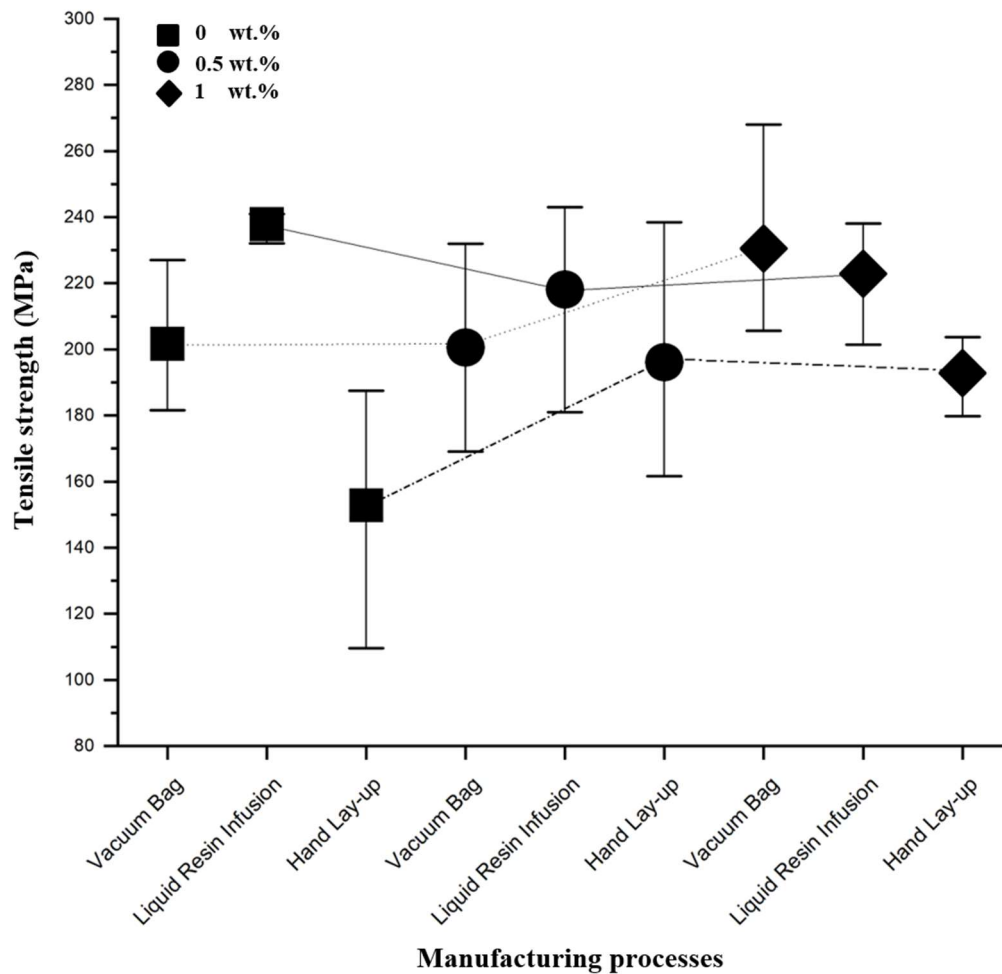


Figure 8. Tensile strength of FRP/MWCNT hybrid laminate for all composites studied.

3.4. Interlaminar shear strength characterization of the FRP/MWCNT hybrid laminate composites

Figure 9 illustrates the apparent interlaminar shear strength behavior of FRP/MWCNTs hybrid laminate composites employing various manufacturing techniques. In Figure 9, the vacuum bag technique exhibits the most substantial enhancement, reaching maximum values of 28 and 35 MPa for 0.5 wt.% and 1 wt.% MWCNTs, respectively (dotted line in Figure 9). These values signify a 65% and 105% increase in apparent interlaminar shear strength compared to the base sample. Conversely, the hand lay-up technique shows a 42% improvement in interlaminar property for 0.5 wt.% MWCNTs, reaching a maximum value of approximately 37 MPa (dash dotted line in Figure 9). However, a parallel

trend to tensile strength results emerges for 1 wt.% MWCNTs, i.e., the presence of primary defects in the technique, such as agglomeration and air bubbles, may contribute to the limited effectiveness of MWCNTs under the mechanical properties of the composites.

In the case of liquid resin infusion, the change in interlaminar behavior is not evident, and one of the main reasons could be the considerations of fluid continuity in the process and the possibility of MWCNTs agglomeration in the final hybrid composites. Moreover, the apparent interlaminar shear strength results are comparable with other authors. Liu et al. [42] obtained apparent interlaminar shear strength results between 35 and 41 MPa for 0.5 wt.% MWCNTs in glass fiber/epoxy composites. Similarly, Chandrasekaran et al. [43] used un-functionalized and functionalized MWCNTs in a 0.5 wt.% concentration with a maximum interlaminar shear strength of 32.25 ± 1.98 and 36.72 ± 3.63 MPa, respectively.

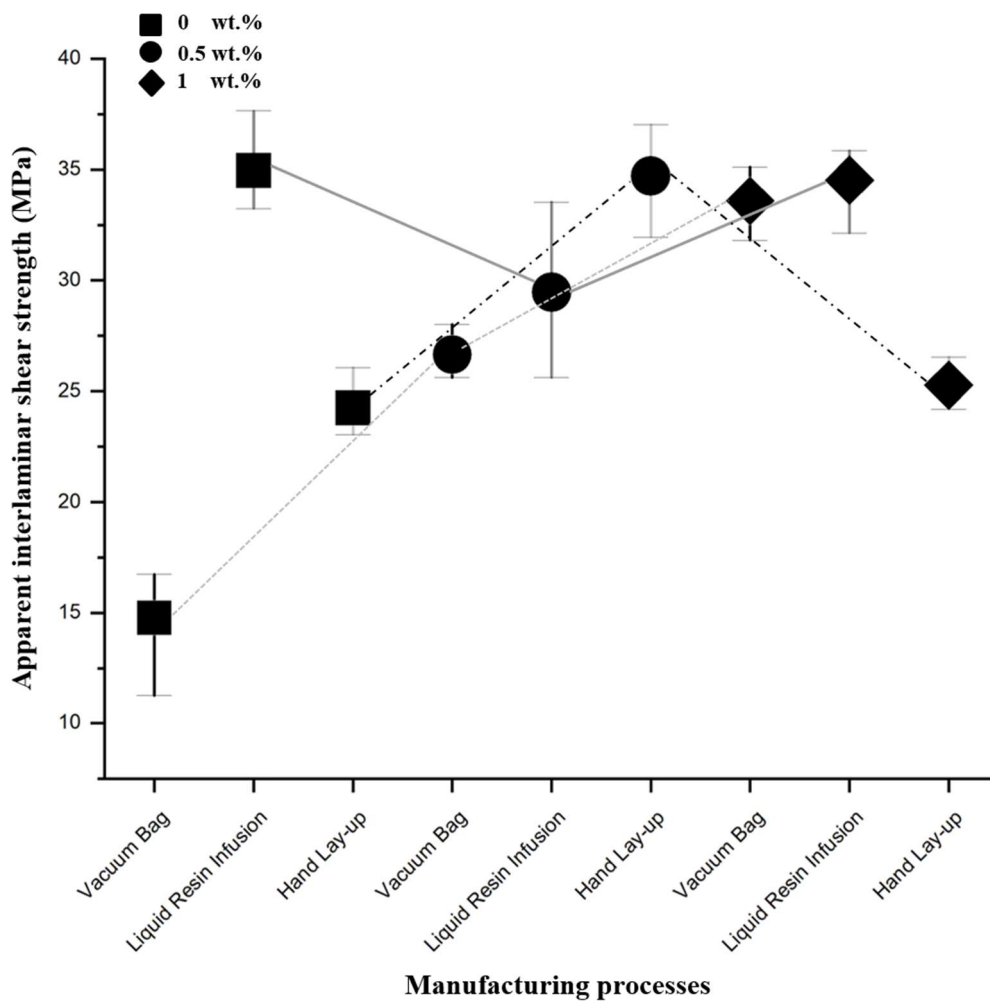


Figure 9. Apparent interlaminar shear strength of FRP/MWCNT hybrid laminate composite.

3.5. Optical and electronical microscopy analysis

In Figure 10, the failures of the hybrid composite materials after the three-point short beam tests for measuring interlaminar strength are observed. In the images of the failures, no differences were found with the amount of MWCNTs added to the polymeric matrix. According to the image of 1% CNTs in Figure 10, the use of different MWCNT contents qualitatively increases crack propagation compared to the base material (0 wt.% MWCNTs). This increase in cracks is particularly evident in the length near the load application point (middle of the sample). Additionally, it is related to the improvement of mechanical properties due to the addition of MWCNTs to the polymeric matrix, i.e., the behavior in the interlaminar zone is fragile. This characteristic may be associated with energy absorption in the materials, enhancing their impact resistance.

Additionally, it can be observed that the stacking sequence has a significant effect on failure. The samples have an unstable behavior (stacking 0-45-90), and crack growth exhibits a failure that propagates between the layers (interlaminar failure), generating multiple failures in the action zone. Despite this, good interlaminar shear strength is shown. This is attributed to the effect provided by the MWCNTs during the generation and growth of a crack, acting as a bridge that prevents or delays the advancement of cracks (bridging effect).

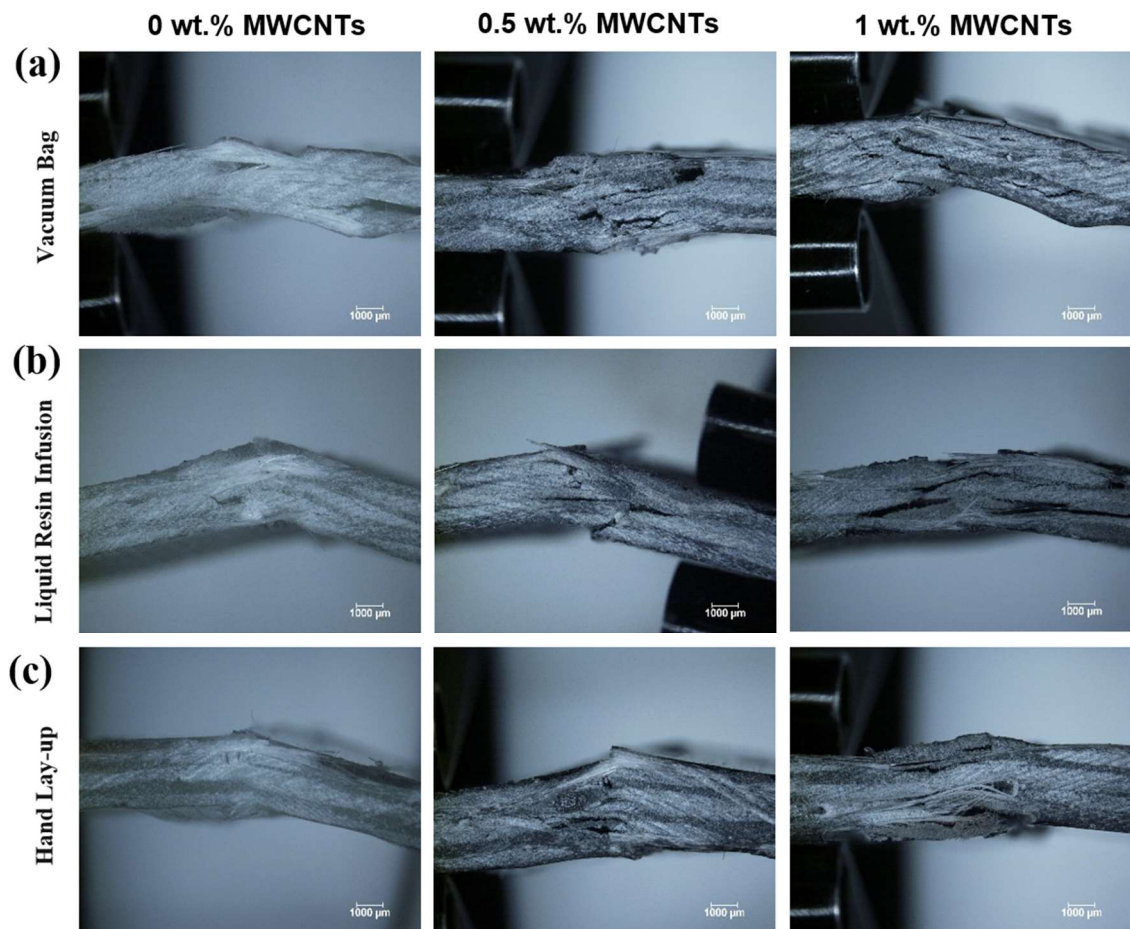


Figure 10. Failures for FRP/MWCNTs hybrid laminate composites manufactured. (a) Vacuum bag, (b) liquid resin infusion and (c) Han lay-up.

SEM images shown in Figure 11 evidence a similar behavior for all manufactured composites. The effect of the nano-reinforcement on the cracks generated during the three-point short beam test is seen. It is evident that the nano-reinforcement shown in Figure 11b,c is covered with a polymer film in its interfacial zone, demonstrating good interaction between the constituents.

In accordance with these results and the previously discussed outcomes, MWCNTs have a significant effect on the interlaminar strength of the manufactured composites, acting as bridges between the layers. Additionally, the image illustrates the type of failure and its initiation (Figure 11a) in the interlaminar zones for the manufactured composites. These failures exhibit characteristics of brittle fractures with well-defined surfaces (Figure 11b,c). At this point, the crack initiates without being influenced by glass fibers or MWCNTs, indicating no bridging effect.

However, as the crack propagates, the glass fiber acts as a bridge, influencing the fracture toughness values [44,45] of the composite due to the instantaneous increase in apparent fracture energy. With the addition of MWCNTs in the matrix, joining the glass fiber and its surroundings, another bridging effect is created, further enhancing the fracture toughness of the composite material. In this specific case, the dispersion of MWCNTs in the matrix, especially in the interlaminar zone, allows for an increase in strength by providing improved characteristics to the matrix (shear strength) [46].

Finally, in the same image, the presence of MWCNTs immersed in the polymeric matrix is evident, demonstrating their immersion in the matrix and the previously demonstrated effect on the mechanical properties of the composite material.

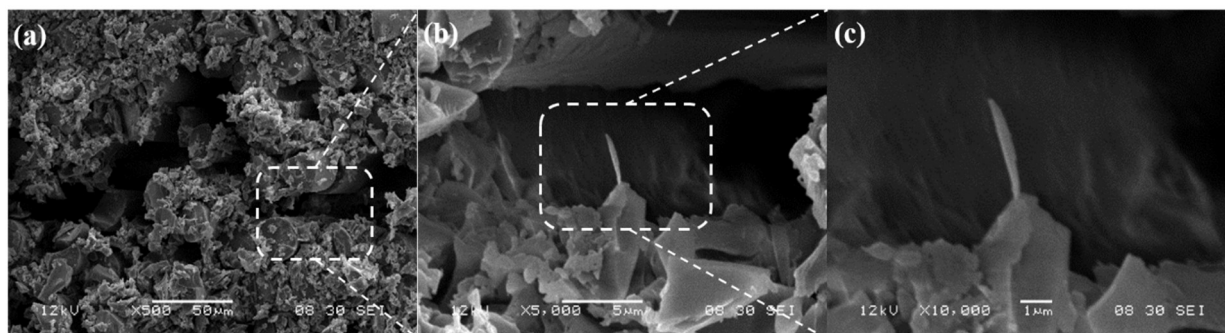


Figure 11. SEM images. (a) Failure of the hybrid composite; (b) detail of the failure in MWCNT; and (c) detail of the MWCNT that acts as a bridge between the sheets.

In summary, the manufacturing processes and the characterization performed show that the addition of carbon nanotubes to the epoxy matrix increases the interlaminar strength of laminated composites, demonstrating that low percentages of nano-reinforcement can have a highly significant effect on the mechanical properties.

4. Conclusions

The study demonstrated that the incorporation of MWCNTs significantly enhanced the mechanical properties and apparent interlaminar shear strength of FRP/MWCNTs hybrid laminate composites. Among the three manufacturing techniques evaluated (hand lay-up, vacuum bag, and liquid resin infusion), the vacuum bag method showed the most significant improvements in apparent

interlaminar shear strength, achieving increases of 65% and 105% for 0.5 and 1 wt.% MWCNTs, respectively. In contrast, liquid resin infusion did not yield significant enhancements, likely due to the re-agglomeration of MWCNTs during resin flow, highlighting the need for effective dispersion control. The dispersion of MWCNTs was quantitatively assessed using the $D_{0.1}$ parameter, which measures the degree of dispersion; composites with 0.5 wt.% MWCNTs had a dispersion degree of 7.9%, while those with 1 wt.% MWCNTs had a higher dispersion degree of 9.2%, indicating better uniformity in the material. Tensile and nanoindentation tests further confirmed the effectiveness of the dispersion methods, contributing to the improved mechanical performance observed. Failure analysis showed that MWCNTs acted as bridges between layers, delaying crack propagation and enhancing impact toughness due to increased crack formation in the interlaminar zone. These findings show the potential of MWCNTs to address interlaminar weaknesses in laminated composite performance in structural applications such as aerospace and automotive industries and suggest that future research should focus on optimizing dispersion techniques and exploring combinations with other nanomaterials. This is due to the manufacturing processes for polymer matrix composite materials using polymer resins such as polyester, vinyl ester, epoxy, and phenolic, among others. Some of these resins have low viscosity, which facilitates the dispersion of nano-reinforcements within the matrix. Additionally, temperature affects viscosity, so processing at elevated temperatures could improve dispersion characteristics. Finally, this type of nano-reinforcement, with a very high aspect ratio (L/d), tends to promote agglomeration; therefore, reinforcements with smaller aspect ratios would contribute to better dispersion within a polymer matrix.

Use of AI tools declaration

The authors declare they have not used Artificial Intelligence (AI) tools in the creation of this article.

Acknowledgments

The authors would like to express their gratitude to Institución Universitaria Pascual Bravo and Universidad Nacional for providing laboratory facilities. CAIM also wishes to acknowledge the support of Universidad de Antioquia for this project. This work was funded through a project approved under the Convocatoria Institucional de Investigación Aplicada para Proyectos de Ciencia y Tecnología (PCT) by Institución Universitaria Pascual Bravo.

Author contributions

Mateo Duarte: writing–review & editing, writing–original draft, methodology, investigation. Johan A. Oquendo: methodology, investigation. Sebastián Vallejo: methodology, investigation. Johnattan Vargas: methodology, conceptualization. Yamile Cardona-Maya: writing–review & editing, writing–original draft, methodology, conceptualization. Cesar A. Isaza: writing–review & editing, validation, supervision, funding acquisition, formal analysis, conceptualization.

Conflict of interest

The authors declare no conflict of interest.

References

1. Bussetta P, Correia N (2018) Numerical forming of continuous fibre reinforced composite material: A review. *Compos Part A Appl Sci Manuf* 113: 12–31. <https://doi.org/10.1016/j.compositesa.2018.07.010>
2. Barile C, Casavola C, De Cillis F (2019) Mechanical comparison of new composite materials for aerospace applications. *Compos B Eng* 162: 122–128. <https://doi.org/10.1016/j.compositesb.2018.10.101>
3. Veeresh Kumar GB, Mageshvar R, Rejath R, et al. (2019) Characterization of glass fiber bituminous coal tar reinforced polymer matrix composites for high performance applications. *Compos B Eng* 175: 107156. <https://doi.org/10.1016/j.compositesb.2019.107156>
4. Zhou K (2021) Composite materials and their fiber reinforcement technology in aerospace field. *SSR* 3: 126–129. <https://doi.org/10.36922/ssr.v3i1.1074>
5. Ballo A, Närhi T (2017) Biocompatibility of fiber-reinforced composites for dental applications, In: Shelton R, *Biocompatibility of Dental Biomaterials*, Cambridge: Woodhead Publishing, 23–39. <https://doi.org/10.1016/B978-0-08-100884-3.00003-5>
6. Sreejith M, Rajeev RS (2021) Fiber reinforced composites for aerospace and sports applications, In: Joseph K, Oksman K, George G, et al. *Fiber Reinforced Composites*, Cambridge: Woodhead Publishing, 821–859. <https://doi.org/10.1016/B978-0-12-821090-1.00023-5>
7. Yadav R, Singh M, Shekhawat D, et al. (2023) The role of fillers to enhance the mechanical, thermal, and wear characteristics of polymer composite materials: A review. *Compos Part A Appl Sci Manuf* 175: 107775. <https://doi.org/10.1016/j.compositesa.2023.107775>
8. Yadav R, Lee HH, Meena A, et al. (2022) Effect of alumina particulate and E-glass fiber reinforced epoxy composite on erosion wear behavior using Taguchi orthogonal array. *Tribol Int* 175: 107860. <https://doi.org/10.1016/j.triboint.2022.107860>
9. Suriani MJ, Rapi HZ, Ilyas RA, et al. (2021) Delamination and manufacturing defects in natural fiber-reinforced hybrid composite: A review. *Polymers* 13: 1323. <https://doi.org/10.3390/polym13081323>
10. Boon Y, Joshi S (2020) A review of methods for improving interlaminar interfaces and fracture toughness of laminated composites. *Mater Today Commun* 22: 100830. <https://doi.org/10.1016/j.mtcomm.2019.100830>
11. Greco F, Leonetti L, Lonetti P (2015) A novel approach based on ALE and delamination fracture mechanics for multilayered composite beams. *Compos B Eng* 78: 447–458. <https://doi.org/10.1016/j.compositesb.2015.04.004>
12. Greco F, Lonetti P, Blasi PN (2007) An analytical investigation of debonding problems in beams strengthened using composite plates. *Eng Fract Mech* 74: 346–372. <https://doi.org/10.1016/j.engfracmech.2006.05.023>
13. Jurf R, Pipes B (1982) Interlaminar fracture of composite materials. *J Compos Mater* 16: 386–394. <https://doi.org/10.1177/002199838201600503>
14. Guo R, Xian GJ, Li CG, et al. (2022) Effect of fiber hybridization types on the mechanical properties of carbon/glass fiber reinforced polymer composite rod. *Mech Adv Mat Struct* 29: 6288–6300. <https://doi.org/10.1080/15376494.2021.1974620>

15. Dasore A, Rajak U, Balijepalli R, et al. (2022) An overview of refinements, processing methods and properties of natural fiber composites. *Mater Today Proc* 49: 296–300. <https://doi.org/10.1016/j.matpr.2021.02.103>
16. Yao ZQ, Wang CG, Qin JJ, et al. (2020) Interfacial improvement of carbon fiber/epoxy composites using one-step method for grafting carbon nanotubes on the fibers at ultra-low temperatures. *Carbon* 164: 133–142. <https://doi.org/10.1016/j.carbon.2020.03.060>
17. Dehrooyeh S, Vaseghi M, Sohrabian M, et al. (2021) Glass fiber/carbon nanotube/epoxy hybrid composites: Achieving superior mechanical properties. *Mech Mat* 161: 104025. <https://doi.org/10.1016/j.mechmat.2021.104025>
18. Tabkhpaz M, Mahmoodi M, Arjmand M, et al. (2015) Investigation of chaotic mixing for MWCNT/polymer composites. *Macromol Mater Eng* 300: 482–496. <https://doi.org/10.1002/mame.201400361>
19. Duongthipthewa A, Su YY, Zhou LM (2020) Electrical conductivity and mechanical property improvement by low-temperature carbon nanotube growth on carbon fiber fabric with nanofiller incorporation. *Compos B Eng* 182: 107581. <https://doi.org/10.1016/j.compositesb.2019.107581>
20. Wu YD, Cheng XY, Chen SY, et al. (2021) In situ formation of a carbon nanotube buckypaper for improving the interlaminar properties of carbon fiber composites. *Mater Des* 202: 109535. <https://doi.org/10.1016/j.matdes.2021.109535>
21. Thakre P, Lagoudas D, Riddick J, et al. (2011) Investigation of the effect of single wall carbon nanotubes on interlaminar fracture toughness of woven carbon fiber-epoxy composites. *J Compos Mater* 45: 1091–1107. <https://doi.org/10.1177/0021998310389088>
22. Nistal A, Falzon B, Hawkins S, et al. (2019) Enhancing the fracture toughness of hierarchical composites through amino-functionalised carbon nanotube webs. *Compos B Eng* 165: 537–544. <https://doi.org/10.1016/j.compositesb.2019.02.001>
23. Nguyen P, Vu X, Ferrier E (2018) Elevated temperature behaviour of carbon fibre-reinforced polymer applied by hand lay-up (M-CFRP) under simultaneous thermal and mechanical loadings: Experimental and analytical investigation. *Fire Saf J* 100: 103–117. <https://doi.org/10.1016/j.firesaf.2018.07.007>
24. Obande W, Brádaigh C, Ray D (2021) Continuous fibre-reinforced thermoplastic acrylic-matrix composites prepared by liquid resin infusion—A review. *Compos B Eng* 215: 108771. <https://doi.org/10.1016/j.compositesb.2021.108771>
25. Muralidhara B, Kumares B, Suresha B (2020) Utilizing vacuum bagging process to prepare carbon fiber/epoxy composites with improved mechanical properties. *Mater Today Proc* 27: 2022–2028. <https://doi.org/10.1016/j.matpr.2019.09.051>
26. Kepple KL, Sanborn GP, Lacasse PA, et al. (2008) Improved fracture toughness of carbon fiber composite functionalized with multi walled carbon nanotubes. *Carbon* 46: 2026–2033. <https://doi.org/10.1016/j.carbon.2008.08.010>
27. Godara A, Mezzo L, Luizi F, et al. (2009) Influence of carbon nanotube reinforcement on the processing and the mechanical behaviour of carbon fiber/epoxy composites. *Carbon* 47: 2914–2923. <https://doi.org/10.1016/j.carbon.2009.06.039>
28. Davis D, Whelan B (2011) An experimental study of interlaminar shear fracture toughness of a nanotube reinforced composite. *Compos B Eng* 42: 105–116. <https://doi.org/10.1016/j.compositesb.2010.06.001>

29. Yu B, Jiang ZY, Tang XZ, et al. (2014) Enhanced interphase between epoxy matrix and carbon fiber with carbon nanotube-modified silane coating. *Compos Sci Technol* 99: 131–140. <https://doi.org/10.1016/j.compscitech.2014.05.021>
30. Wicks S, Wang WN, Williams M, et al. (2014) Multi-scale interlaminar fracture mechanisms in woven composite laminates reinforced with aligned carbon nanotubes. *Compos Sci Technol* 100: 128–135. <https://doi.org/10.1016/j.compscitech.2014.06.003>
31. Yokozeki T, Iwahori Y, Ishiwata S, et al. (2007) Mechanical properties of CFRP laminates manufactured from unidirectional prepregs using CSCNT-dispersed epoxy. *Compos Part A Appl Sci Manuf* 38: 2121–2130. <https://doi.org/10.1016/j.compositesa.2007.07.002>
32. Sheth D, Maiti S, Patel S, et al. (2021) Enhancement of mechanical properties of carbon fiber reinforced epoxy matrix laminated composites with multiwalled carbon nanotubes. *Fullerenes Nanotubes Carbon Nanostruct* 29: 288–294. <https://doi.org/10.1080/1536383x.2020.1839424>
33. Rathore D, Prusty R, Kumar D, et al. (2016) Mechanical performance of CNT-filled glass fiber/epoxy composite in in-situ elevated temperature environments emphasizing the role of CNT content. *Compos Part A Appl Sci Manuf* 84: 364–376. <https://doi.org/10.1016/j.compositesa.2016.02.020>
34. Tugrul S, Tanoglu M, Schulte K (2008) Mode I and mode II fracture toughness of E-glass non-crimp fabric/carbon nanotube (CNT) modified polymer based composites. *Eng Fract Mech* 75: 5151–5162. <https://doi.org/10.1016/j.engfracmech.2008.08.003>
35. Fan ZH, Santare MH, Advani SG (2008) Interlaminar shear strength of glass fiber reinforced epoxy composites enhanced with multi-walled carbon nanotubes. *Compos Part A Appl Sci Manuf* 39: 540–554. <https://doi.org/10.1016/j.compositesa.2007.11.013>
36. Joshi SC, Dikshit V (2011) Enhancing interlaminar fracture characteristics of woven CFRP prepreg composites through CNT dispersion. 46: 665–675. <https://doi.org/10.1177/0021998311410472>
37. Medina S, Isaza C, Meza J, et al. (2015) Mechanical and thermal behavior of polyvinyl alcohol reinforced with aligned carbon nanotubes. *Matéria* 20: 794–802. <https://doi.org/10.1590/S1517-707620150003.0085>
38. Tiwari M, Billing B, Bedi H, et al. (2020) Quantification of carbon nanotube dispersion and its correlation with mechanical and thermal properties of epoxy nanocomposites. *J Appl Polym Sci* 137: 48879. <https://doi.org/10.1002/APP.48879>
39. Avella M, Errico ME, Martelli S, et al. (2001) Preparation methodologies of polymer matrix nanocomposites. *Appl Organomet Chem* 15: 435–439. <https://doi.org/10.1002/aoc.168>
40. Lillehei P, Kim JW, Gibbons L, et al. (2009) A quantitative assessment of carbon nanotube dispersion in polymer matrices. *Nanotechnology* 20: 325708. <https://doi.org/10.1088/0957-4484/20/32/325708>
41. Siddiqui N, Li E, Sham ML, et al. (2010) Tensile strength of glass fibres with carbon nanotube-epoxy nanocomposite coating: Effects of CNT morphology and dispersion state. *Compos Part A Appl Sci Manuf* 41: 539–548. <https://doi.org/10.1016/j.compositesa.2009.12.011>
42. Liu Y, Yang JP, Xiao HM, et al. (2012) Role of matrix modification on interlaminar shear strength of glass fibre/epoxy composites. *Compos B Eng* 43: 95–98. <https://doi.org/10.1016/j.compositesb.2011.04.037>

43. Chandrasekaran VCS, Advani SG, Santare MH (2011) Influence of resin properties on interlaminar shear strength of glass/epoxy/MWNT hybrid composites. *Compos Part A Appl Sci Manuf* 42: 1007–1016. <https://doi.org/10.1016/j.compositesa.2011.04.004>
44. Lee J, Lim J, Huh J (2000) Mode II interlaminar fracture behavior of carbon bead-filled epoxy/glass fiber hybrid composite. *Polym Compos* 21: 343–352. <https://doi.org/10.1002/pc.10191>
45. Albertsen H, Ivens J, Peters P, et al. (1995) Interlaminar fracture toughness of CFRP influenced by fibre surface treatment: Part 1. Experimental results. *Compos Sci Technol* 54: 133–145. [https://doi.org/10.1016/0266-3538\(95\)00048-8](https://doi.org/10.1016/0266-3538(95)00048-8)
46. Wang PF, Zhang X, Lim GH, et al. (2015) Improvement of impact-resistant property of glass fiber-reinforced composites by carbon nanotube-modified epoxy and pre-stretched fiber fabrics. *J Mater Sci* 50: 5978–5992. <https://doi.org/10.1007/s10853-015-9145-3>



AIMS Press

© 2024 the Author(s), licensee AIMS Press. This is an open access article distributed under the terms of the Creative Commons Attribution License (<https://creativecommons.org/licenses/by/4.0>)